International Journal of Applied Earth Observation and Geoinformation 33 (2014) 203–210

Contents lists available at ScienceDirect

International Journal of Applied Earth Observation and Geoinformation

journal homepage: www.elsevier.com/locate/jag

Estimating soil sand content using thermal infrared spectra in arid lands

Mamat Sawut[a,b,c], Abduwasit Ghulam[a,c], Tashpolat Tiyip[b,*], Yan-jun Zhang[a], Jian-li Ding[a,b], Fei Zhang[a,b], Matthew Maimaitiyiming[c]

[a] College of Resources and Environmental Sciences, Xinjiang University, Urumqi, Xinjiang 830046, China
[b] Ministry of Education Key Laboratory of Oasis Ecology at Xinjiang University, Urumqi, Xinjiang 830046, China
[c] Center for Sustainability, Saint Louis University, Saint Louis, MO 63103, USA

ARTICLE INFO

Article history:
Received 28 February 2014
Accepted 23 May 2014

Keywords:
Thermal infrared spectra
Emissivity
Sand content

ABSTRACT

Sand content is a textural property of soils closely related to soil quality. A fast determination of sand content at large scales is paramount importance for monitoring soil degradation to improve agricultural practices. The main objective of this study is to evaluate the ability of the thermal infrared region (TIR) to estimate sand content of soils. Thermal infrared spectra obtained in the field from a Fourier Transform Spectrometer are used to develop a partial least square regression model (PLSR) that translates thermal emittance to soil texture properties. Our results show that the 9.435–9.473 μm wavelength regions hold a great promise for prediction of sand content. Coefficient of determination R^2 is 0.87 and standard error (SE) is 2.79. We also show that second derivative of thermal spectral profiles is very useful to detect kaolinite in sand dominated soils. The results of this study provide further insights for developing future thermal sensors aimed at predicting soil quality as indicated by the sand content and other textural properties.

Introduction

Sustainable and profitable soil management requires reliable, and timely information on soil properties that determines soil usage (Carter, 2002; Kempen et al., 2012; Ray, 2001). The physical properties of soils including texture, structure, density, porosity, consistency, temperature, color and resistivity are often used in soil erosion modeling, crop suitability assessment, land degradation monitoring, and environmental risk assessment (Larson et al., 1985; Goldshleger et al., 2010; Goncalves and Carlyle, 1994; Merckx et al., 1990; Rey et al., 2011; Sgouras et al., 2007; Vrieling et al., 2008). The soil texture is the most important property of soils, and is determined by the relative proportion of the three types of soil particles, i.e., sand, silt, and clay. Among those, sand is the textural property closely related to soil quality (Andrade et al., 2013). Sandy soils are more vulnerable to drought than clay soils, storing less water and likely to lose water more rapidly by plant growth (Miller, 2004; Ray, 2001). Also this type of soils holds few nutrients and loses them easily as water moves through the soil (Goncalves and Carlyle, 1994). Knowledge of the spatial distribution of sand content including other properties is important to monitor and map areas vulnerable to desertification, and increased soil erosion (Kosmas et al., 2006). There is, therefore, a great need for up to date, accurate, and timely information on sand content. Large scale mapping and analyzing soils for their textural properties typically involves extensive field work and laboratory techniques that are time consuming (Abdu et al., 2008; Chang and Islam, 2000; Hewson et al., 2012). Remote sensing has become a promising tool in monitoring soil quality and related environmental issues over the past decades thanks to its rapid, non-destructive and cost-effective capabilities (Beeri and Peled, 2009; Chopping et al., 2006; Khawlie et al., 2002; Li et al., 2012; Mougenot et al., 1993; Platt and Sathyendranath, 2008; Tralli et al., 2005; Wiens et al., 2009; Zhang and Zhang, 2007). An increasing number of studies have emphasized the ability of remote sensing for monitoring the soil physical properties (Palacios-Orueta and Ustin, 1998; Ben-Dor, 2002; Shepherd and Walsh, 2002), soil engineering properties (e.g., expansiveness) (Chabrillat et al., 2013; Yitagesu et al., 2009, 2011), soil salinity (Farifteh et al., 2007; Metternicht et al., 2005), soil erosion (Luleva et al., 2013) and soil quality (Cécillon et al., 2009). Its potential for determining soil textural properties within visible (VIS: 0.4–0.7 μm), near infrared (NIR: 0.7–1.1 μm) shortwave infrared (SWIR: 1.1–2.5 μm) ranges

* Corresponding author. Tel.: +(86) 991-858-1186; fax: +(86) 991-858-1186.
E-mail address: tash@xju.edu.cn (T. Tiyip).

http://dx.doi.org/10.1016/j.jag.2014.05.010
0303-2434/

has been investigated (Ben-Dor and Banin, 1995; Casa et al., 2013; Shepherd and Walsh, 2002; Viscarra Rossel et al., 2006; Zornoza et al., 2008). Soil texture affects the spectral reflectance of the soils due to its influence on water holding capacity and the size of soil particles (Barnes et al., 2003; Casa et al., 2013; Hassink, 1994; Numata et al., 2003; Scott Bechtold and Naiman, 2006; Skaggs et al., 2001). Sandy soil exhibits higher reflectance than that of clay soil due to the abundance of macro pores and air-soil interface that cause multiple reflection/scattering. Efficacy of the technique in estimating clay content has also been demonstrated using near infrared remote sensing (NIRS) (Al-Abbas et al., 1972; Ben-Dor and Banin, 1995; Chang et al., 2001; Moron and Cozzolino, 2003; Zornoza et al., 2008).

Water and organic matter is typically low in sand dominated soils. Although sand content is one of the most important factors controlling spectral signatures of the soil, VNIR-SWIR region is less sensitive to Si—O related components (Eisele et al., 2012; Salisbury et al., 1991). In contrast, thermal infrared (TIR: 8–14 μm) region may contain diagnostic information on silicate minerals in sand rich soil. This is due to the presence of vibrational frequencies of silicate and carbonate molecules that elicit differences in the spectral emissivity of soils (Rubio et al., 1997; Salisbury and D'Aria, 1992a). Moreover, the texture variability of sand rich soils is high, which enables the reststrahlen bands between 8 and 12 μm regions to provide detailed soil textural information (Eisele et al., 2012). A laboratory analysis indicated that discriminating the quartz or silicate content of soils requires spectral information within the mid- (3–5 μm) and the thermal-infrared wavelength regions (7–14 μm) (Salisbury and D'Aria, 1992b). Despite these promises and demonstrated potentials of using TIR regions in determining soil texture properties, fundamentals of interactions between thermal spectra and sand content have been poorly understood. It is imperative that conceptual and operational approaches for TIR remote sensing of sand content needs to be developed.

The objective of this study is to examine the feasibility of predicting sand content using a partial least squares regression (PLSR) analysis between soil sand content and TIR spectral signatures. The possibility of inferring soil quality as indicated by sand content is also explored by using first and second derivative indices of thermal infrared spectra. The work was carried out in several steps including: (1) soil samples were collected in the field for laboratory determination; (2) spectral data were obtained from these samples using Fourier Transform Spectrometer in the field; (3) PSLR model was developed for predicting soil sand content; (4) the performance of PLSR models in predicting the sand content and soil quality was examined using first and send derivative spectral indices.

Data and methods

Study site

The study area is located at the northern foot of the Kunlun Mountains along the edge of the Taklimakan Desert (81°09′–82°51′E, 35°14′–39′29N) in Northwestern China's Xinjiang Uyghur Autonomous Region (Fig. 1). Geomorphology of the area is characterized by desert with active dunes and sand seas, desert pediment with fans, and foothills with deep gorges and glaciated mountains. The landforms and sediments in this region are polygenetic in origin, being transported, eroded and deposited by glacial, fluvial, Aeolian and lacustrine processes (Yang et al., 2002). The soil in the region contains 50% sand-size particles with the rest consisting of impurities such as feldspar, mica, and cement of silica, iron or carbonates. Most of the soils are coarse in texture, acid, deep, and low in nutrients.

The continental climate of this region is characterized by severe weather conditions. From the north to the south, the annual precipitation decrease significantly from 195 mm to 44 mm, and the annual mean temperature ranging from 4.7 °C to 11.2 °C (Yuquan, 1990). The region entirely depends on the Keriya River, which vanishes in the sands of the Taklimakan desert (Yang, 2001). Since the 1950, the Keriya River has been intensely exploited. Today, the area is suffering severe water shortages under excessive pressure from population increase, agricultural expansion and most importantly from the steady encroachment of desertification (Hong et al., 2012). The vegetation varies considerably depending on water condition along the Keriya River, which include spare brush vegetation and halophilic plants (Yuquan, 1990).

Soil sampling and particle size analysis

Fieldwork was conducted in August 2012 during a dry season. 25 sites were selected for soil sampling (Fig. 1), which covers a wider range of soil characteristics. At each site, five samples were taken from the topsoil (0–30 cm) on a regular grid of 30 m intervals. In total, 125 samples were collected for laboratory analysis. The soil samples were air-dried, and sieved through 2 mm sieves, prepared by chemically removing salts, organic matter, expected the particle size difference to play a larger role on soil emissivity. Care was taken to ensure that no samples had any soil moisture or organic matter content remained so that their difference between the samples would have a negligible effect on soil texture and soil emissivity. To determine soil sand content, we analyzed soil samples for the particle size distribution using MICROTRAC S3500 Particle Size Analyser. The particle-size distribution was determined using U.S. Department of Agriculture (USDA) textural soil classification system, which defines the size of clay (<0.002 mm), silt (0.002–0.05 mm) and sand (0.05–2.0 mm) (Skaggs et al., 2001). The Microtrac S3500 uses laser diffraction technology to provide accurate, reliable particle size information. It has a measurement range of 0.02–2800 μm. Detailed description of laser diffraction method (LDM) can be found in Di Stefano et al. (2010).

Soil spectral measurements

Soil radiances were measured using Designs and Prototypes (D & P), Inc. Mycroft model 102 Fourier Transform Spectrometer. It is a portable field spectrometer that covers 2–16 μm wavelengths with a spectral resolution of 4 cm^{-1}. With a fore optic of a 4.8° field of view, the ground field of view is approximately 20 mm at 650 mm height. The instrument was equipped with a liquid-nitrogen-cooled two element detector (dual InSb/MCT). Measurements were calibrated to radiance units ($W/m^2/sr/\mu m$) using hot and cold black body measurements. The FT-IR instrument was always placed at a fixed position during the measurements. To obtain the spectral emissivity of each sample, four raw data files are required; three are for calibration (warm blackbody, cold blackbody, downwelling radiance) and one is sample surface radiance. The blackbodies (warm blackbody and cold blackbody) are used to calibrate the sample surface radiance and downwelling radiances. The downwelling radiance data is collected from a diffuse reflector. Emissivity was measured on clear days without cloud cover and no wind. In addition, we performed a series of measurements typically within about each 10 min. During the measurements, temperatures of the fore-optics, diffuse reflector, the air, and the sample surface were collected with thermistors to detect any changes in the thermal environmental conditions that affect the accuracy of

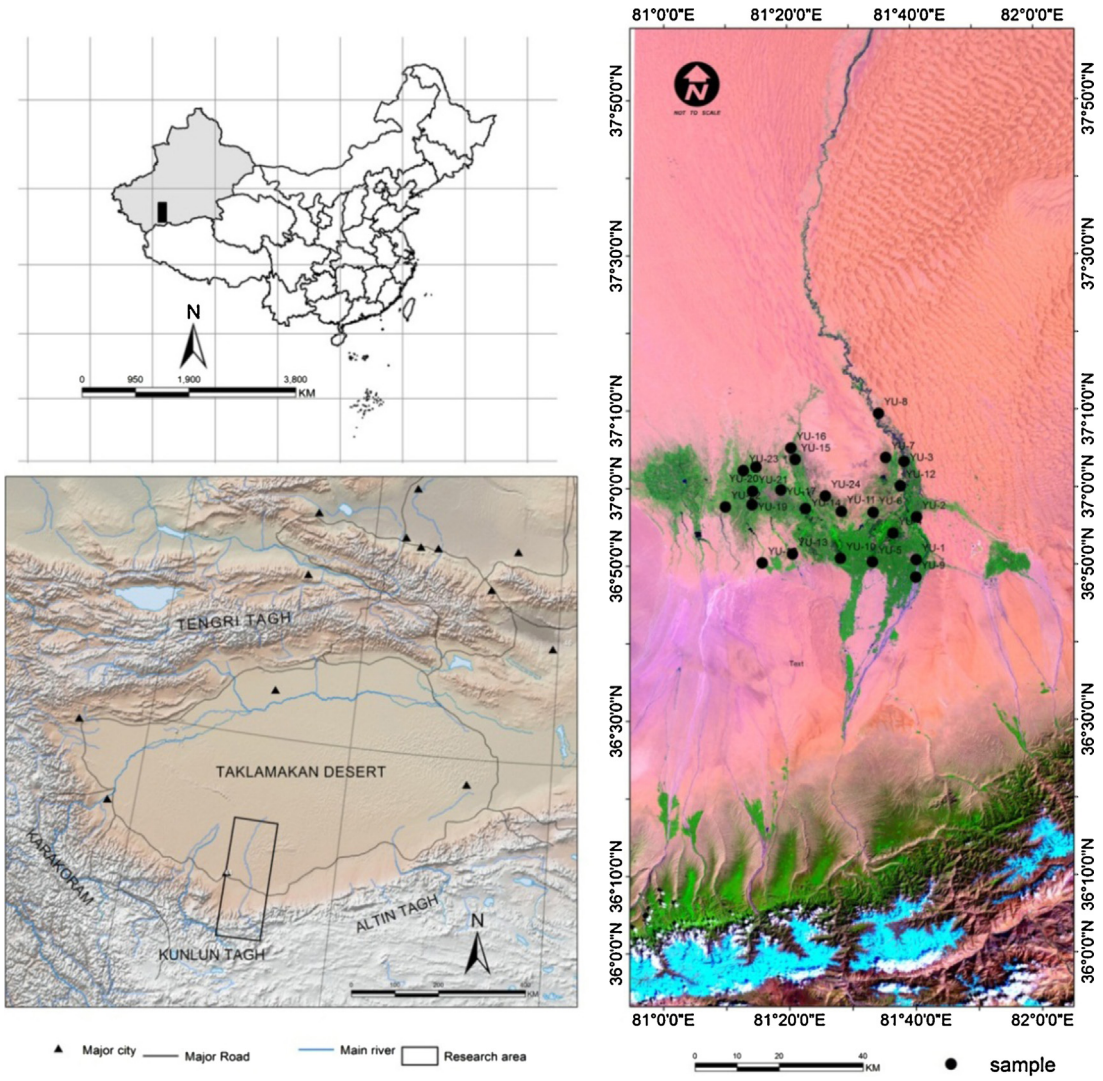

Fig. 1. The location map of the study area. Black triangles in the left-bottom image represents major cities. The image to the left is color composite (7, 4, 2 in RGB) derived from Landsat ETM+ data and black solid circles represent sampling locations.

the measurements. The algorithm used to compute the emissivity is given by Johnson et al. (1998) and Salisbury et al. (1994).

$$\varepsilon_S(\lambda) = \frac{L_s(\lambda) - l_{DW}(\lambda)}{B(T_S, \lambda) - l_{DW}(\lambda)} \tag{1}$$

where $\varepsilon_S(\lambda)$ is the surface emissivity of the sample as a function of wavelength; $L_S(\lambda)$ is the calibrated radiance of the sample; $l_{DW}(\lambda)$ is the calibrated radiance of the downwelling radiance; $B(T_S, \lambda)$ is a Planck function at the sample temperature. Eq. (1) requires the soil surface temperature is known, which can be determined by a least-square analysis aimed to minimize the spectral smoothness measure below (Ingram and Muse, 2001):

$$S = \sum_{j=2}^{N-1} \left(j - \frac{j-1+j+j+1}{3} \right)^2 \tag{2}$$

where εj is the emissivity at the j band, N is the band number. The estimated surface temperature is then taken to be the temperature that yields the smoothest emissivity curve (Fig. 2). We found the temperature value by iteration of the value that minimizes the spectral smoothness measure (Fig. 3).

Statistical analyses

Statistical analyses are often used to extract the information about the soil attributes that is hidden within the spectral information. Essentially, this involves regression techniques coupled

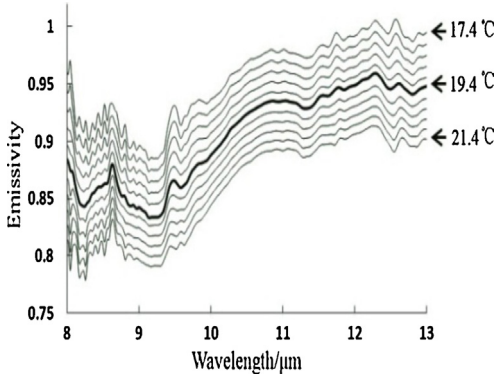

Fig. 2. Emissivity calculated using the 11 different temperature levels ranging from 17.4 °C to 21.4 °C at the 0.4 °C intervals. The solid curve represents the best fit to emissivity estimation obtained from spectral smoothness method.

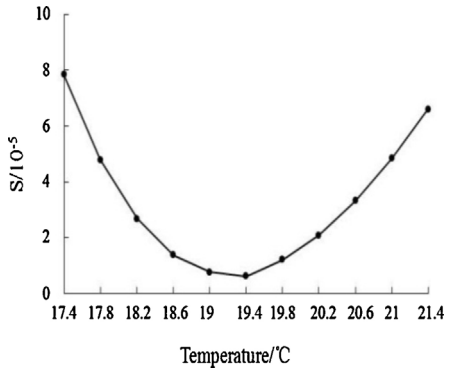

Fig. 3. Illustration of the spectral smoothness principle. The best spectral smoothness coefficient was obtained at the temperature of 19.4 °C.

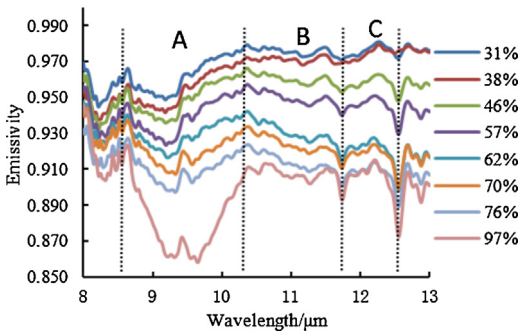

Fig. 4. Thermal spectral variations of soil with different levels of sand content: showing spectrally responsive regions.

with spectral preprocessing (Ben-Dor, 2002; Dehaan and Taylor, 2002; Farifteh et al., 2007). Firstly, spectral separability of different sand content was determined. For a spectrum consists of many highly correlated neighboring wavelengths, the spectral correlation vectors were generated in order to capture spectral information that may strongly relate to sand content. Coefficient of determination (R^2) was estimated by sequential regression of spectra ratios against sand content. Larger R^2 in positive or negative values indicate spectral bands are sensitive, and have a positive or negative relationships with the predicted soil sand content. The bands with highest coefficient of determination values are selected as the measurement bands for the final sand content predictive model. We used five prior to partial least square regression model (PLSR) analyses including reciprocal, logarithm, standard normal variety (SNV), first-derivative (1st-d), second-derivative (2nd-d) spectra of samples (Wetterlind et al., 2013; Yang et al., 2002). Next, we applied PLSR to predict sand content. PLSR is a multivariate regression method that specifies a linear relationship between a set of dependent (response) variables, Y, and a set of predictor variables, X (Haaland and Thomas, 1988). As a powerful tool specifically designed to deal with the data consisting of many independent variables and reduce collinearity within the data like the thermal infrared spectra (Martens and Naes, 1996; Wold et al., 2001), this approach has been proven to be effective in quantifying the relationship between soil properties and spectral data (Udelhoven et al., 2003; Yang et al., 2003). Detailed description of the PLSR analyses can be found in Geladi and Kowalski (1986) and Wold et al. (2001). We also use quadratic and exponential model to examine a possible nonlinear relationship between sand content in soils and thermal spectra. Finally, we examined the model performance by comparing the coefficient of determination (R^2), and standard error (SE) calculated from both calibration and validation dataset. The dataset were divided into two subsets, one for building the model (50 samples) and one for validation (20 samples). The R^2 indicate strength of statistical correlation between measured values and predicted values for models, and SE indicate estimation errors (Taylor, 1997). The T test is carried out using a significance level of 5%, $\alpha = 0.05$ for the significance of regression.

Results

Soil analyses

Based on the laboratory analysis of the 50 samples used for modeling, the sand content were between 27.32% and 93.21%, and clay content varied between 2.32% and 10.53%. For the validation samples sand content ranged from 23.45% to 96.63%, and the clay content from 3.65% to 11.62%. Particle size measurements showed that the majority of the samples were composed of coarse grained quartz, while the few samples contained a mixture of clay-sized minerals of kaolinite and feldspar. The results indicated that the soil samples represented a general characteristics of soil textural properties in the study area.

Spectral analysis

Both the overall shape of the spectrum and absorption bands is important in explaining the spectral properties of soils (Ben-Dor and Banin, 1995). Fig. 4 presents the emissivity spectra for the soil samples that sand content varies from 30% to 95%. We observed that the emissivity and spectral contrast differ across the 8.6–10.3 μm (A), 10.3–11.7 μm (B) and 11.7–12.5 μm (C) wavelength regions (Fig. 4). In region A, the absorption features are broad, formed two asymmetric absorption bands at near 9.4 μm wavelengths with a great spectral contrast. Whereas, near 8.5 μm which is located just before start of the region A, there appears another absorption feature. However, the spectral responses to the change in sand content were relatively less significant as can be seen from overlapped spectral shapes. In region B, spectra showed a moderate differences indicating sensitivity to smaller or medium amount of sand content. In region C, the absorption features were narrow and sharp, appearing at near 11.7 μm and 12.5 μm. Smaller spectral differences were observed for samples with small or larger sand content.

Notably, the results showed that the 8.6–10.3 μm region provides overall separability of soil samples with different sand content. This may be resulted from the scattering properties of the sand dominated soil in which Si—O cations have strong fundamental molecular vibrations in the reststrahlen (7.5–12.3 μm) bands than in any other portion of the TIR spectrum. In general, the reststrahlen features in thermal infrared, soil spectra exhibit trends in position, strength, and number of features that are diagnostic of the relative proportions of the Si and O cations in the soil minerals (Salisbury et al., 1991; Salisbury and D'Aria, 1992b). Fig. 4 shows that the different sand content is distinct in this spectral region. Overall, these results demonstrated that there is a spectral region that can be used to infer sand contents with statistical significance.

Correlations between sand content and spectra

Fig. 5 shows the relationship between the correlation coefficient and emissivity spectra derived from different processing algorithms. It is evident from Fig. 5 that the best performing wavelength spans 8.6–10.3 μm regions. Larger R^2 were found over larger portions of this region. The observed general trend is that diagnostic band positions were shifting to this region with increasing sand content, which located in the reststrahlen bands (Fig. 5a). The correlations between sand content and spectral data are summarized in Table 2. Among the different processing algorithms, largest R^2

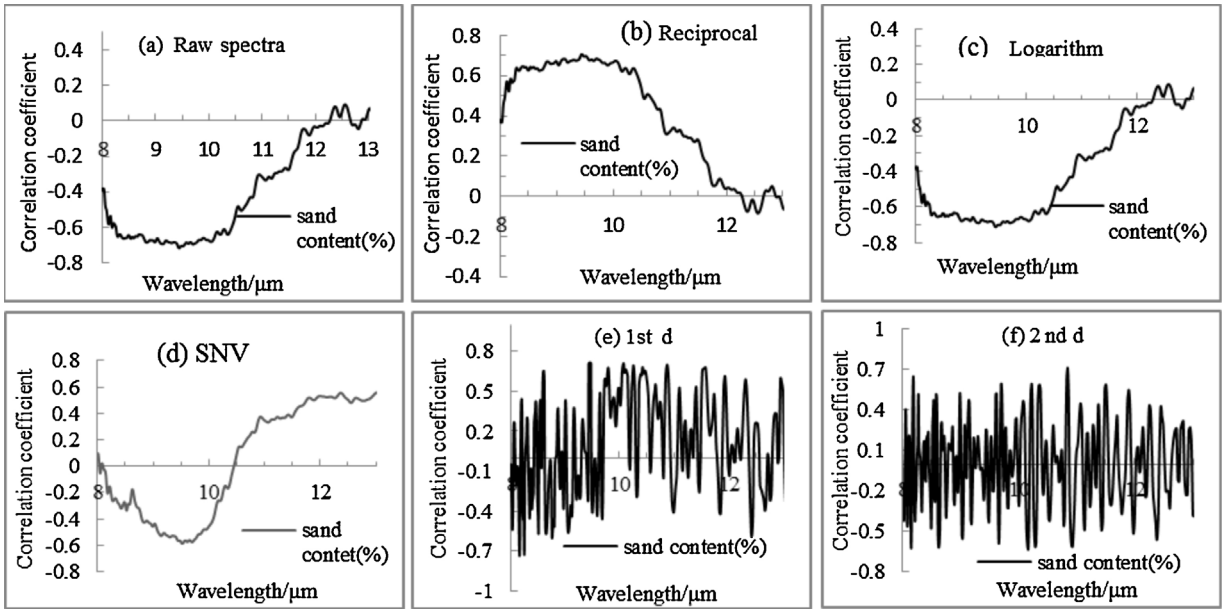

Fig. 5. Relative spectral of correlation coefficient of sand content: (a) raw spectra; (b) reciprocal; (c) logarithm; (d) standard normal variety (SNV); (e) first derivative (1st d); (f) second derivative (2nd d).

Table 1
Descriptive statistics for the soil samples.

Data	Soil property	Min	Max	Mean	Standard deviation
Data set for model developing	Sand (%)	27.32	93.21	81.73	4.25
	Clay (%)	2.32	10.53	7.27	2.21
Data set for validation	Sand (%)	23.45	96.63	84.52	3.47
	Clay (%)	3.65	11.62	8.34	3.35

were found with the raw spectra and 1st derivative. In particularly, the largest correlations between the spectra and sand content were located in 9.422–9.473 μm range with peak at 9.447 μm, indicating potential for estimation of sand content. It is worth to mention that the 11.0–13 μm regions were no sensitive to sand content.

While the correlation regression with reciprocal, logarithm, standard normal variety (SNV) and first-derivative (1st-d) spectra uncovered additional, subtle spectral features contributing to the sand content predictions, the second derivative (2nd-d) spectra was useful to find important spectral features related to clay minerals (Table 1 and Fig. 5f). 2nd-d correlation for sand content was concentrated in the 10.824–10.858 μm ranges with peak at 10.841 μm and 10.824 μm (Fig. 5f). The latter 2nd-d features are associated with the presence of clay minerals, such as kaolinite (China Clay), which occurred in our soil samples.

The key finding of the correlation regression study was that sand contents are directly linked to the emissivity spectra that make different sand content spectrally distinct, 2nd-d derivative spectral features can help to find clay minerals in soil. We thus conclude that a soil thermal infrared signature is closely associated with sand content, and the 9.435–9.447 μm range is best for delineating different sand content. This is important for mapping soil quality, particularly to tackle key soil related environmental threats such as soil erosion, land degradation and plant growth potential.

Table 2
Descriptive statistics of correlation analysis between spectra and sand content.

Pre-treatments	Maximum correlated (spectra/μm)	Coefficients of determination $\|R^2\|$
Raw spectra	9.447	0.72
Reciprocal	9.445	0.71
Logarithm	9.434	0.71
Standard normal variety (SNV)	9.550	0.59
First derivative (1st d)	9.472	0.72
Second derivative (2 nd d)	10.841	0.71

Model calibration and validation

Table 3 and Fig. 6 summarize the PLSR model performance for estimation of sand content. Compared to Exponential (Fig. 6a) and Quadratic (Fig. 6c) models, the best fit was found with the PLS model (Fig. 6b). Fig. 6b shows the predicted versus measured sand content for this models. For both calibration and validation dataset, significant correlations and predictive power were achieved with the R^2 values of 0.88 and 0.87, respectively. This is also indicated by the low SE values as shown in Table 3. As mentioned before, the higher sand content prediction accuracy can be attributed to scattering properties of soil.

The calibration dataset showed a slightly better prediction results (R^2 = 0.88 and SE = 2.54), while the R^2 values of validation dataset were lower (R^2 = 0.87 and SE = 2.79). The correlations between measured and estimated sand content using PLSR model are illustrated in Fig. 7. The predictive power of the model was demonstrated by R^2 of 0.88. Also the p-value for the both dataset is lower than the common alpha level of 0.05, which indicates the results are statistically significant.

In addition, we compared this PLSR model to nonlinear regression models. Using exponential and quadratic model did not improve the model performance. The SE are generally higher (Table 3). The poor sand content estimations based on these models are presumably related to linear relationship between sand content and spectra. Overall, these results indicated that PLSR model is useful in sand content predictions.

Table 3
Performance statistics of PLSR calibration models.

Datasets	Model type	x	Model	R^2	SE
Calibration	Exponential	9.434–9.473 μm	$y = 0.3945e^{8E-6x}$		3.88
	Quadratic		$y = -3 * 10^{-11} \times^2 + 6 * 10^{-6}x + 0.5462$		3.47
	PLS		$y = 7 * 10^{-6}x + 0.5106$	0.878	2.54
Validation	PLS		$y = 0.6446x + 0.2026$	0.869	2.69

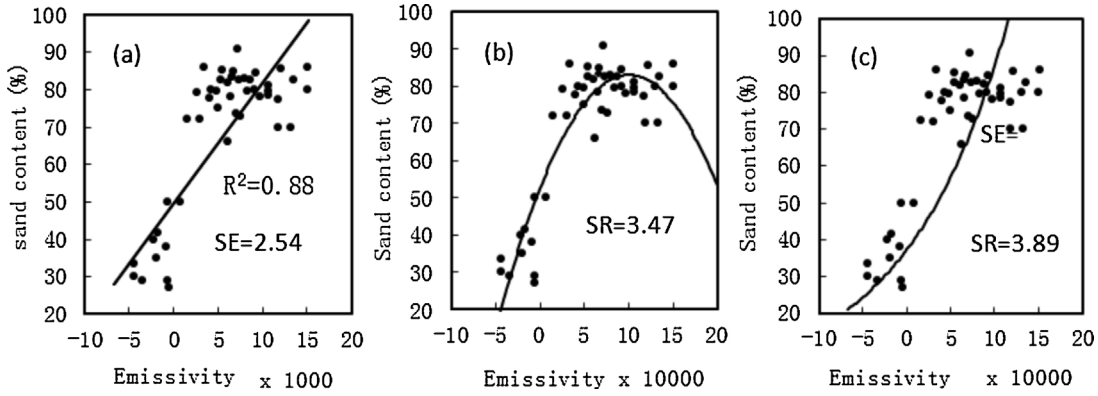

Fig. 6. Model of emissivity spectra for predicting sand content: (a) PLSR model; (b) quadratic model; (c) exponential model.

Discussion

The study area is dominated by an undulating sand plain system, and ours samples included few clay soil samples commonly found in the area of investigation. The soil consists predominantly of quartz with clays, resulting in characteristic restrahlen band in the 8.0–9.5 μm region. The thermal infrared spectral regions (3–5 μm and 8–14 μm) contains information on quartz, feldspars, silicate minerals, mafic, clay, carbonate mineral group, and organic compounds (Chabrillat et al., 2013). As expected, the relationship between sand content and soil emissivity in the TIR regions demonstrated positive and negative peaks of correlation coefficients (Fig. 5). It also showed that the 8.0–9.5 μm is the important spectral regions for the prediction of sand content, which fit with the occurrence of the most distinctive spectral features for this wavelength. Derivation of clay mineral content, sand content, and organic carbon content was performed based on indices derived from the TIR region using the 9.5 μm, 8.62 μm, and 3.45 μm spectral features, respectively (Hewson et al., 2012). A good correlation with mineral content was observed for the quartz index, which demonstrated the added value of the TIR region (emissivity) to the VNIR-SWIR region (Hewson et al., 2012).

Commonly used spectral pre-treatments include the 1st and 2nd Derivatives, which has practical advantages for PLSR analyses (Buddenbaum and Steffens, 2012). In our study, four different spectral pre-treatments were tested, but the influence of the different pre-treatments on the spectral analyses was found to be small. Although several authors noted the benefit of transforming spectra before further analyses (Udelhoven et al., 2003; Stenberg and Viscarra Rossel, 2010; Rossel and Chen, 2011), these pretreatments were not helpful except for the 2nd derivatives. This is probably due to the fact that pre-treatment methods are designed for baseline corrections, and their effect is minimal when the baseline variance is small (Buddenbaum and Steffens, 2012).

A number of statistical regression approaches were evaluated for their pros and cons to predict soil spectral properties by Viscarra Rossel et al. (2006). Among these methods, the PLSR is more robust, and commonly used (Vohland and Emmerling, 2011). The statistics of estimated sand content as given in Table 3 show how well the variable can be predicted from emissivity data by using the

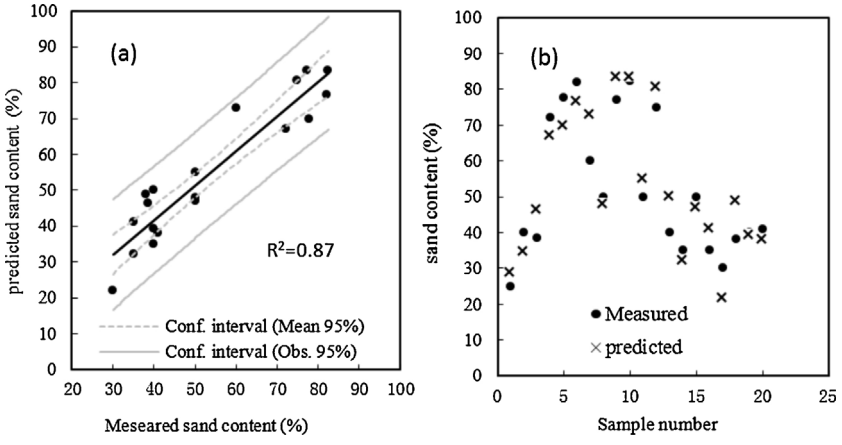

Fig. 7. (a) Validation using a validation dataset for the PLSR spectral model; (b) scatter plot of measured values and predicted values with the PLSR.

PLSR model. The prediction power of sand content can be considered good, because the R^2 values are higher than 0.8. For the validation dataset, more than 95% of variations are explained by the emissivity variable (Fig. 7a). The poor soil sand content estimations from the nonlinear model (see Table 3) was probably due to (1) there exist stronger linear relationship between sand content and spectra, or (2) the selected model could not capture the nonlinear relationship. Other nonlinear calibration models, for example neural networks (NN), might be explored since it showed a great potential for estimating and mapping salt-affected soil, clay content and soil organic matter (SOM) (Farifteh et al., 2007; Yang et al., 2003).

The interest on determining soil textural properties including composition of sand, clay and silt should be high as predictive mapping of areas vulnerable to desertification and/or soil erosion has become on of the critical issues under changing climate., typically demonstrated by increased soil erosion (Hewson et al., 2012). The challenge is that it typically requires extensive field work and laboratory analysis, and therefore large scale observation of soil textural parameters are extremely difficult unless otherwise utilizing remote sensing techniques. With recent developments in TIR remote sensing, the chance of the prediction of soil textural properties continues to grow (Ben-Dor and Banin, 1995).

Conclusion

Research, conservation and management efforts are calling for methods to map, monitor and predict the soil properties to understand their impact on soil quality. Thermal infrared remote sensing is a potential tool for mapping soil properties; however, efforts are needed to generalize methods and algorithms capable of carrying out this task. We presented a study of the spectral separability of the most common soil properties found in arid and semi-arid regions using thermal infrared sensing. Also, we investigated the possibilities of TIR wavelength region to quantitatively derive sand content in soils.

Our study showed that the 9.435–9.473 μm regions hold the promise of greater prediction accuracy for predicting soil sand content. Among the Exponential, Quadratic and PLSR models employed in this contribution, the PLSR model was identified as the most potential predictive model of sand content. Best predictive results were achieved using TIR spectral signatures in this region with a R^2 of 0.87 and a SE of 2.79. We also found that second derivative of thermal infrared spectra is useful to detect kaolinite in soils. The results of this study demonstrated that thermal infrared data provide a useful tool for predicting the sand content in soil that commonly occurs in arid region.

Although the approach presented here was based on field measurements of sand content and thermal spectra, it provides meaningful insights to predict and map sand content over large geographical region using TIR satellite imagery, which is critical in designing future thermal sensors.

Acknowledgments

This research was jointly funded by the National Natural Science Foundation of China (No. 41361016, No. U1138302, U1303381 and No. 41130531), Research Foundation of XinJiang University (No. BS120116, No. XY110117 and No. BS110125), and Education Department of Xinjiang Uyghur Autonomous Region (No. XJEDU2011S07 and No. XJEDU2012S03), The Department of Science and Technology of Xinjiang Uyghur Autonomous Region, China (No. 2013711014). We would like to extend our sincere thanks for the anonymous reviewers of this manuscript for their helpful suggestions.

References

Abdu, H., Robinson, D., Seyfried, M., Jones, S.B., 2008. Geophysical imaging of watershed subsurface patterns and prediction of soil texture and water holding capacity. Water Resour. Res., 44.
Al-Abbas, A., Swain, P., Baumgardner, M., 1972. Relating organic matter and clay content to the multispectral radiance of soils. Soil Sci. 114, 477–485.
Andrade, F., Mendonça, E., Silva, I., 2013. Organic acids and diffusive flux of organic and inorganic phosphorus in sandy-loam and clayey latosols. Commun. Soil Sci. Plant Anal. 44, 1211–1223.
Barnes, E.M., Sudduth, K.A., Hummel, J.W., Lesch, S.M., Corwin, D.L., Yang, G., Doughtry, C., Bausch, W.C., 2003. Remoe-and ground-based sensor techniques to map soil properties. Photogramm. Eng. Remote Sens. 69, 619–630.
Beeri, O., Peled, A., 2009. Geographical model for precise agriculture monitoring with real-time remote sensing. ISPRS J. Photogramm. Remote Sens. 64, 47–54.
Ben-Dor, E., 2002. Quantitative remote sensing of soil properties. Adv. Agron. 75, 173–243.
Ben-Dor, E., Banin, A., 1995. Near-infrared analysis as a rapid method to simultaneously evaluate several soil properties. Soil Sci. Soc. Am. J. 59, 364–372.
Buddenbaum, H., Steffens, M., 2012. The effects of spectral pretreatments on chemometric analyses of soil profiles using laboratory imaging spectroscopy. Appl. Environ. Soil Sci. 2012, 1–12.
Carter, M.R., 2002. Soil quality for sustainable land management. Agron. J. 94, 38–47.
Casa, R., Castaldi, F., Pascucci, S., Palombo, A., Pignatti, S., 2013. A comparison of sensor resolution and calibration strategies for soil texture estimation from hyperspectral remote sensing. Geoderma 197, 17–26.
Cécillon, L., Barthès, B.G., Gomez, C., Ertlen, D., Genot, V., Hedde, M., Stevens, A., Brun, J.-J., 2009. Assessment and monitoring of soil quality using near-infrared reflectance spectroscopy (NIRS). Eur. J. Soil Sci. 60, 770–784.
Chabrillat, S., Ben-Dor, E., Rossel, R.A.V., Demattê, J.A.M., 2013. Quantitative soil spectroscopy. Appl. Environ. Soil Sci. 3, 1–3.
Chang, C.-W., Laird, D.A., Mausbach, M.J., Hurburgh, C.R., 2001. Near-infrared reflectance spectroscopy – principal components regression analyses of soil properties. Soil Sci. Soc. Am. J. 65, 480–490.
Chang, D.-H., Islam, S., 2000. Estimation of soil physical properties using remote sensing and artificial neural network. Remote Sens. Environ. 74, 534–544.
Chopping, M., Su, L., Laliberte, A., Rango, A., Peters, D.P., Kollikkathara, N., 2006. Mapping shrub abundance in desert grasslands using geometric-optical modeling and multi-angle remote sensing with CHRIS/Proba. Remote Sens. Environ. 104, 62–73.
Dehaan, R., Taylor, G., 2002. Field-derived spectra of salinized soils and vegetation as indicators of irrigation-induced soil salinization. Remote Sens. Environ. 80, 406–417.
Di Stefano, C., Ferro, V., Mirabile, S., 2010. Comparison between grain-size analyses using laser diffraction and sedimentation methods. Biosyst. Eng. 106, 205–215.
Eisele, A., Lau, I., Hewson, R., Carter, D., Wheaton, B., Ong, C., Cudahy, T.J., Chabrillat, S., Kaufmann, H., 2012. Applicability of the thermal infrared spectral region for the prediction of soil properties across semi-arid agricultural landscapes. Remote Sens. 4, 3265–3286.
Farifteh, J., Van der Meer, F., Atzberger, C., Carranza, E., 2007. Quantitative analysis of salt-affected soil reflectance spectra: a comparison of two adaptive methods (PLSR and ANN). Remote Sens. Environ. 110, 59–78.
Geladi, P., Kowalski, B.R., 1986. Partial least-squares regression: a tutorial. Anal. Chim. acta 185, 1–17.
Goldshleger, N., Ben-Dor, E., Lugassi, R., Eshel, G., 2010. Soil degradation monitoring by remote sensing: examples with three degradation processes. Soil Sci. Soc. Am. J. 74, 1433–1445.
Goncalves, J., Carlyle, J., 1994. Modelling the influence of moisture and temperature on net nitrogen mineralization in a forested sandy soil. Soil Biol. Biochem. 26, 1557–1564.
Haaland, D.M., Thomas, E.V., 1988. Partial least-squares methods for spectral analyses. 1. Relation to other quantitative calibration methods and the extraction of qualitative information. Anal. Chem. 60, 1193–1202.
Hassink, J., 1994. Effect of soil texture on the size of the microbial biomass and on the amount of C and N mineralized per unit of microbial biomass in Dutch grassland soils. Soil Biol. Biochem. 26, 1573–1581.
Hewson, R.D., Cudahy, T.J., Jones, M., Thomas, M., 2012. Investigations into soil composition and texture using infrared spectroscopy. Appl. Environ. Soil Sci., 12.
Ingram, P.M., Muse, A.H., 2001. Sensitivity of iterative spectrally smooth temperature/emissivity separation to algorithmic assumptions and measurement noise. IEEE Trans. Geosci. Remote Sens. 39, 2158–2167.
Johnson, J.R., Lucey, P.G., Horton, K.A., Winter, E.M., 1998. Infrared measurements of pristine and disturbed soils 1. Spectral contrast differences between field and laboratory data. Remote Sens. Environ. 64, 34–46.
Kempen, B., Brus, D.J., Stoorvogel, J.J., Heuvelink, G., de Vries, F., 2012. Efficiency comparison of conventional and digital soil mapping for updating soil maps. Soil Sci. Soc. Am. J. 76, 2097–2115.
Khawlie, M., Awad, M., Shaban, A., Bou Kheir, R., Abdallah, C., 2002. Remote sensing for environmental protection of the eastern Mediterranean rugged mountainous areas, Lebanon. ISPRS J. Photogramm. Remote Sens. 57, 13–23.
Kosmas, C., Tsara, M., Moustakas, N., Kosma, D., Yassoglou, N., 2006. Environmentally sensitive areas and indicators of desertification. In: Kepner, W., Rubio, J., Mouat, D., Pedrazzini, F. (Eds.), Desertification in the Mediterranean Region. A Security Issue. Springer, Netherlands, pp. 525–547.

Hong, L., L., X.H., Qing qing, Z., 2012. Nonlinear analysis of runoff change and climate factors in the headstream of Keriya River, XinJiang. Geogr. Res. 31.
Larson, W.E., Fenton, T.E., Skidmore, E.L., Benbrook, C.M., 1985. Effects of soil erosion on soil properties as related to crop productivity and classification. In: Follett, R.F., Stewart, B.A. (Eds.), Soil Erosion and Crop Productivity. Amer. SOC. Agron, Madison, WI, pp. 189–211.
Li, D., Durand, M., Margulis, S.A., 2012. Potential for hydrologic characterization of deep mountain snowpack via passive microwave remote sensing in the Kern River basin, Sierra Nevada, USA. Remote Sens. Environ. 125, 34–48.
Luleva, M.I., van der Werff, H., van der Meer, F., Jetten, V., 2013. Observing change in potassium abundance in a soil erosion experiment with field infrared spectroscopy. Chem.: Bulg. J. Sci. Educ. 22 (1), 91–109.
Martens, H., Naes, T., 1996. Multivariate Calibration. John Wiley and Sons Ltd., Co., New York.
Merckx, R., Smolders, E., Vlassak, K., 1990. The soil to plant transfer of nutrients: combining plant and soil characteristics. In: Beusichem, M.L. (Ed.), Plant Nutrition – Physiology and Applications. Springer, Netherlands, pp. 3–8.
Metternicht, G., Hurni, L., Gogu, R., 2005. Remote sensing of landslides: an analysis of the potential contribution to geo-spatial systems for hazard assessment in mountainous environments. Remote Sens. Environ. 98, 284–303.
Miller, D.T.G.A.R.W., 2004. Soils in Our Environment: Upper Saddle River, 10th ed. Prentice Hall PTR, New Jersey.
Moron, A., Cozzolino, D., 2003. Exploring the use of near infrared reflectance spectroscopy to study physical properties and microelements in soils. J. Near Infrared Spec. 11, 145–154.
Mougenot, B., Pouget, M., Epema, G., 1993. Remote sensing of salt affected soils. Remote Sens. Rev. 7, 241–259.
Numata, I., Soares, J., Roberts, D., Leonidas, F., Chadwick, O., Batista, G., 2003. Relationships among soil fertility dynamics and remotely sensed measures across pasture chronosequences in Rondônia, Brazil. Remote Sens. Environ. 87, 446–455.
Palacios-Orueta, A., Ustin, S.L., 1998. Remote sensing of soil properties in the Santa Monica Mountains I. Spectral analysis. Remote Sens. Environ. 65, 170–183.
Platt, T., Sathyendranath, S., 2008. Ecological indicators for the pelagic zone of the ocean from remote sensing. Remote Sens. Environ. 112, 3426–3436.
Ray, N.C.B.a.R.W., 2001. The Nature and Properties of Soils: Upper Saddle River. Prentice Hall, New Jersey.
Rey, A., Pegoraro, E., Oyonarte, C., Were, A., Escribano, P., Raimundo, J., 2011. Impact of land degradation on soil respiration in a steppe (*Stipa tenacissima* L.) semi-arid ecosystem in the SE of Spain. Soil Biol. Biochem. 43, 393–403.
Rossel, R.A.V., Chen, C., 2011. Digitally mapping the information content of visible-near infrared spectra of surficial Australian soils. Remote Sens. Environ. 115, 1443–1455.
Rubio, E., Caselles, V., Badenas, C., 1997. Emissivity measurements of several soils and vegetation types in the 8–14 μm wave band: analysis of two field methods. Remote Sens. Environ. 59, 490–521.
Salisbury, J.W., D'Aria, D.M., 1992a. Emissivity of terrestrial materials in the 8–14 μm atmospheric window. Remote Sens. Environ. 42, 83–106.
Salisbury, J.W., D'Aria, D.M., 1992b. Infrared (8–14 μm) remote sensing of soil particle size. Remote Sens. Environ. 42, 157–165.
Salisbury, J.W., Wald, A., D'Aria, D.M., 1994. Thermal-infrared remote sensing and Kirchhoff's law: 1. Laboratory measurements. J. Geophys. Res.: Solid Earth (1978–2012) 99, 11897–11911.
Salisbury, J.W., Walter, L.S., Vergo, N., D'Aria, D.M., 1991. Infrared (2.1–25 micrometers) Spectra of Minerals. Johns Hopkins University Press, Baltimore, Maryland.
Scott Bechtold, J., Naiman, R.J., 2006. Soil texture and nitrogen mineralization potential across a riparian toposequence in a semi-arid savanna. Soil Biol. Biochem. 38, 1325–1333.
Sgouras, I., Tsadilas, C., Barbayiannis, N., Danalatos, N., 2007. Physicochemical and mineralogical properties of red Mediterranean soils from Greece. Commun. Soil Sci. Plant Anal. 38, 695–711.
Shepherd, K.D., Walsh, M.G., 2002. Development of reflectance spectral libraries for characterization of soil properties. Soil Sci. Soc. Am. J. 66, 988–998.
Skaggs, T., Arya, L., Shouse, P., Mohanty, B., 2001. Estimating particle-size distribution from limited soil texture data. Soil Sci. Soc. Am. J. 65, 1038–1044.
Stenberg, B., Viscarra Rossel, R.A., 2010. Diffuse reflectance spectroscopy for high-resolution soil sensing. In: Viscarra Rossel, R.A., McBratney, B.A., Minasny, B. (Eds.), Proximal Soil Sensing. Springer Science + Business, Dordrecht, The Netherlands, pp. 29–47.
Taylor, J.R., 1997. An Introduction to Error Analysis: The Study of Uncertainties in Physical Measurements. University Science Books, Sausalito, California.
Tralli, D.M., Blom, R.G., Zlotnicki, V., Donnellan, A., Evans, D.L., 2005. Satellite remote sensing of earthquake, volcano, flood, landslide and coastal inundation hazards. ISPRS J. Photogramm. Remote Sens. 59, 185–198.
Udelhoven, T., Emmerling, C., Jarmer, T., 2003. Quantitative analysis of soil chemical properties with diffuse reflectance spectrometry and partial least-square regression: a feasibility study. Plant Soil 251, 319–329.
Viscarra Rossel, R., Walvoort, D., McBratney, A., Janik, L.J., Skjemstad, J., 2006. Visible, near infrared, mid infrared or combined diffuse reflectance spectroscopy for simultaneous assessment of various soil properties. Geoderma 131, 59–75.
Vohland, M., Emmerling, C., 2011. Determination of total soil organic C and hot water-extractable C from VIS–NIR soil reflectance with partial least squares regression and spectral feature selection techniques. Eur. J. Soil Sci. 62, 598–606.
Vrieling, A., De Jong, S.M., Sterk, G., Rodrigues, S.C., 2008. Timing of erosion and satellite data: a multi-resolution approach to soil erosion risk mapping. Int. J. Appl. Earth Observ. Geoinform. 10, 267–281.
Wetterlind, J., Stenberg, B., Rossel, R.A.V., 2013. Soil analysis using visible and near infrared spectroscopy. In: Plant Mineral Nutrients. Springer, pp. 95–107.
Wiens, J., Sutter, R., Anderson, M., Blanchard, J., Barnett, A., Aguilar-Amuchastegui, N., Avery, C., Laine, S., 2009. Selecting and conserving lands for biodiversity: the role of remote sensing. Remote Sens. Environ. 113, 1370–1381.
Wold, S., Sjöström, M., Eriksson, L., 2001. PLS-regression: a basic tool of chemometrics. Chemom. Intell. Lab. Syst. 58, 109–130.
Yang, H., Griffiths, P.R., Tate, J., 2003. Comparison of partial least squares regression and multi-layer neural networks for quantification of nonlinear systems and application to gas phase Fourier transform infrared spectra. Anal. Chim. Acta 489, 125–136.
Yang, X., 2001. The oases along the Keriya River in the Taklamakan Desert, China, and their evolution since the end of the last glaciation. Environ. Geol. 41, 314–320.
Yang, X., Zhu, Z., Jaekel, D., Owen, L., Han, J., 2002. Late quaternary palaeoenvironment change and landscape evolution along the Keriya River, Xinjiang, China: the relationship between high mountain glaciation and landscape evolution in foreland desert regions. Quatern. Int. 97, 155–166.
Yitagesu, F.A., van der Meer, F., van der Werff, H., Seged, H., 2011. Evaluation of soil expansion index from routinely determined geotechnical parameters. Soil Sci. Soc. Am. J. 75, 1640–1651.
Yitagesu, F.A., van der Meer, F., van der Werff, H., Zigterman, W., 2009. Quantifying engineering parameters of expansive soils from their reflectance spectra. Eng. Geol. 105 (3–4), 151–160.
Yuquan, L., 1990. The climatic characteristics and its changing tendency in the Taklimakan desert. J. Desert Res. 2, 001.
Zhang, J., Zhang, Y., 2007. Remote sensing research issues of the national land use change program of China. ISPRS J. Photogramm. Remote Sens. 62, 461–472.
Zornoza, R., Guerrero, C., Mataix-Solera, J., Scow, K., Arcenegui, V., Mataix-Beneyto, J., 2008. Near infrared spectroscopy for determination of various physical, chemical and biochemical properties in Mediterranean soils. Soil Biol. Biochem. 40, 1923–1930.